

Cogenesis of baryon and dark matter with PBH and QCD axion

Debasish Borah,^{1,*} Nayan Das,^{1,†} Suruj Jyoti Das,^{2,‡} and Rome Samanta^{3,4,5,§}

¹*Department of Physics, Indian Institute of Technology Guwahati, Assam 781039, India*

²*Particle Theory and Cosmology Group,*

Center for Theoretical Physics of the Universe,

Institute for Basic Science (IBS), Daejeon, 34126, Korea

³*CEICO, Institute of Physics of the Czech Academy of Sciences,*

Na Slovance 1999/2, 182 21 Prague 8, Czech Republic

⁴*Scuola Superiore Meridionale, Largo S. Marcellino 10, I-80138 Napoli, Italy*

⁵*Istituto Nazionale di Fisica Nucleare (INFN),*

sez. di Napoli, Via Cinthia 9, I-80126 Napoli, Italy

Abstract

With entropy injection, an early matter-dominated epoch (EMD) impels the axion decay constant f_a towards larger values to produce correct axion dark matter (DM) abundance, thereby unfolding the low-mass axion ($m_a \lesssim 10^{-5}$ eV) parameter space to be searched for in axion experiments. We implement this proposition in a scenario where f_a and the leptogenesis scale in a seesaw mechanism are equivalent. We show, that if instead, the EMD is provided by evaporating ultralight primordial black holes (PBH), the scenario becomes strikingly testable with gravitational waves (GW) background alongside the axion searches. In particular, while being consistent with correct axion DM abundance, the scale $f_a \gtrsim 10^{12}$ GeV, corresponding to the unflavored regime of leptogenesis with hierarchical right-handed neutrinos, can be probed with GW and axion experiments, which is otherwise not testable at neutrino or collider experiments. Additionally, axions produced from PBH evaporation can give rise to dark radiation within reach of future cosmic microwave background experiments.

*Electronic address: dborah@iitg.ac.in

†Electronic address: nayan.das@iitg.ac.in

‡Electronic address: surujjd@gmail.com

§Electronic address: romesamanta@gmail.com

I. INTRODUCTION

Strong upper limits on the electric dipole moment of neutron show that strong interactions are CP symmetric [1], although the standard model (SM) entirely is not. The CP violation in the strong interaction is characterized by the angle $\bar{\theta}$, which is bounded from above: $\bar{\theta} < 10^{-10}$. The required vanishingly small value of the $\bar{\theta}$ parameter is the origin of the strong-CP problem. The classic solution to this is to promote $\bar{\theta}$ as a pseudoscalar axion field resulting from a global $U(1)$ symmetry breaking – the Peccei-Quinn (PQ) mechanism [2–5]. When the axion field acquires its potential through QCD effects, remarkably, $\bar{\theta}$ relaxes to zero (ground state of the potential) and solves the strong-CP problem. Besides solving the strong-CP problem, axion could constitute the entire cold dark matter (DM) energy density if they are sufficiently light $m_a \simeq 10^{-5}$ eV [6–8]. The key UV parameter in any QCD axion model is the scale of the PQ symmetry breaking f_a , also known as the axion decay constant. In the models of light QCD axions, f_a is bounded from below by astrophysical observations as $f_a \gtrsim 10^8$ GeV [9, 10]. On the other hand, the vacuum misalignment mechanism offers a stringent window¹ for the decay constant around $f_a \sim 10^{11}$ GeV to produce the correct dark matter relic [15]. This simple PQ solution to the strong-CP problem thus renders dark matter physics and evades astrophysical constraints, generically for a high-scale phase transition corresponding to the PQ symmetry breaking. Since there exist other observed phenomena which the SM fails to explain, one might wonder whether any other cosmological puzzles attributed to high-scale physics in their simplest theoretical form share common ground with axion physics.

This article discusses one such possibility, where the generation of the baryon asymmetry of the Universe (BAU) through thermal leptogenesis [16] shares a common origin with axion physics. While there are several ways in which one couples the axion physics to the baryogenesis [17–20], our interest aligns with the SMASH-like [21] scenarios (and similar extensions [22, 23]). In this scenario, the right-handed neutrinos (RHN) introduced in the SM to generate light neutrino mass via seesaw mechanism and to provide leptogenesis, get mass from the PQ phase transition, i.e., $f_a \equiv M \equiv \Lambda_{\text{lepto}}$, where $M(\Lambda_{\text{lepto}})$ is the RHN mass,

¹ Depending on the IR models, e.g., Dine-Fischler-Srednicki-Zhitnitsky (DFSZ) [11, 12] and Kim-Shifman-Vainshtein-Zakharov (KSVZ) [13, 14], additional contributions from the topological defects can alter this window by less than an order of magnitude [15].

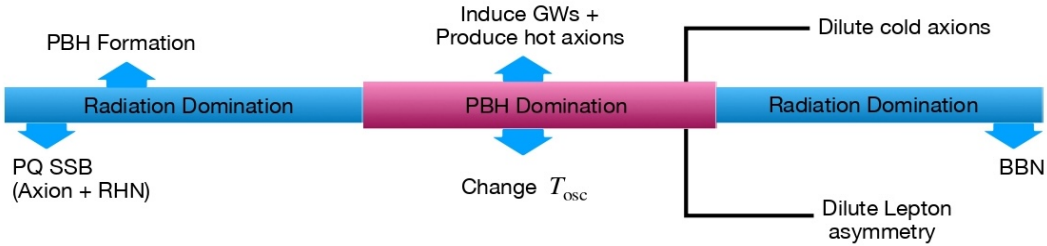


FIG. 1: Schematic diagram showing a possible timeline of the scenario.

equivalent to the scale of seesaw and thermal leptogenesis. Such a unification therefore addresses neutrino mass, strong-CP problem, DM, and BAU at one stroke. Unlike Ref.[21] for SMASH-like frameworks, the main motivation to unify the leptogenesis scale Λ_{lepto} and the PQ scale f_a in this work is to explore the testability of $\Lambda_{\text{lepto}} \equiv f_a \gtrsim 10^{12}$ GeV—also referred to as the vanilla regime of leptogenesis². On the other hand, for $f_a \gtrsim 10^{12}$ GeV, axion dark matter gets overproduced via vacuum misalignment mechanism with standard cosmological expansion. In order not to lose the interesting connection among axion DM, strong-CP problem and vanilla leptogenesis, we explore the possibility that before the big bang nucleosynthesis (BBN), the Universe underwent an early matter-dominated phase releasing entropy while reproducing the standard radiation dominated Universe [29, 30].

In this work, we show that if the matter domination is provided by ultralight evaporating primordial black holes (PBH) [31–33] with initial mass $m_{\text{in}} \lesssim 3.4 \times 10^8$ g, testability enhances significantly. This is because, in addition to predicting axion parameter space in the $g_{\alpha\gamma} - m_a$ plane, one can have stochastic gravitational waves (GWs) signatures via PBH density fluctuations [34–38]. Remarkably, the mass range of PBH required to generate correct DM and at the same time BAU, produces GWs within the frequency bands of current and planned GW detectors. A schematic diagram of this scenario showing a possible timeline is presented in Fig. 1. Two additional (not mentioned so far) features in this figure namely, the axion oscillation temperature T_{osc} and the production of hot axions in the form of dark radiation within reach of future cosmic microwave background (CMB) experiments are discussed later in this article.

² Recently there have been some efforts to probe high-scale leptogenesis (including vanilla regime) with primordial gravitational waves e.g., topological defects [24–28].

Let us also add the following remarks.

- Production of axion DM with PBH-induced matter domination has been studied in Ref.[39, 40]. The crucial difference here nonetheless is that, because we implemented the PBH-induced matter domination in SMASH-like scenarios, the requirement of generating the observed baryon asymmetry restricts the model parameter space severely to predict constrained GW-signal in amplitude as well as in frequency (see, e.g., Eq.(16), (22), and Fig.4). As such, a hierarchical (resonant) leptogenesis scenario would predict weaker (stronger) GWs with detectable peak frequencies varying within the mHz-Hz range.

- Given the early Universe before BBN epoch is unknown, the motivation to introduce PBH-induced pre-BBN matter domination in this work is purely phenomenological; as recently explored in a plethora of works, see, e.g., Refs.[39–58] related to DM models, and Refs. [31, 50–53, 59–68] for baryogenesis models. While PBH might arise owing to different (independent of the framework discussed here) new physics [33, 69–71], a self-consistent framework would be to explore the formation of ultralight PBH in this model itself, e.g., via domain wall collapse [72]. We, however, do not explore such a possibility here.

The rest of the paper is organized as follows. In sec.II, we briefly discuss the particle physics framework we have adopted in this work. The interplay of axion DM and leptogenesis in the presence of PBH is presented in sec.III. In sec.IV, we discuss the detection prospect of the framework in GW and axion experiments. We conclude in sec.V.

II. THE FRAMEWORK

We consider a type-I seesaw framework [73–77] extended by Peccei-Quinn symmetry [2, 3]. A recent review of QCD axion models can be found in [78]. In addition to the heavy RHNs (here we consider three RHNs) required for the seesaw, the other field content and PQ charges are kept similar to a KSVZ type model [13, 14] in which $v_{\text{PQ}} = f_a$, where v_{PQ} is the vacuum expectation value (VEV) of the PQ scalar field σ and f_a is the axion decay constant³. Thus, the BSM field content is constituted by a complex PQ scalar field $\sigma \equiv \frac{v_{\text{PQ}} + \rho}{\sqrt{2}} e^{ia/f_a}$ ($\sigma \sim (1, 1, 0)$), a heavy quark $Q \sim (3, 1, 0)$ and three right-handed

³ It should be noted that our particle content is same as the SMASH framework [21]. While SMASH considers Higgs portal inflation via non-minimal coupling to gravity, we remain agnostic about the origin of inflation.

neutrinos $N_R \sim (1, 1, 0)$ where the numbers in brackets denote their charges under the SM gauge symmetry $SU(3)_c \times SU(2)_L \times U(1)_Y$. The transformation of these fields and leptons under PQ symmetry are

$$\sigma \rightarrow e^{i\alpha} \sigma; \quad N_R \rightarrow e^{-i\alpha/2} N_R; \quad l_R, L \rightarrow e^{-i\alpha/2} l_R, L; \quad Q_L \rightarrow e^{i\alpha/2} Q_L; \quad Q_R \rightarrow e^{-i\alpha/2} Q_R.$$

The SM quarks have vanishing PQ charges. The Yukawa coupling part of the PQ invariant Lagrangian can be written as

$$\mathcal{L}_Y = - \left[y \bar{Q}_L \sigma Q_R + G_{ij} \bar{L}_i H l_{jR} + F_{ij} \bar{L}_i \tilde{H} N_{jR} + \frac{1}{2} y_{ij} \bar{N}_{iR}^c \sigma N_{jR} \right] + \text{h.c.} \quad (1)$$

with H being the SM Higgs. The scalar potential of the model is given by

$$V(H, \sigma) = \lambda_H \left(H^\dagger H - \frac{v^2}{2} \right)^2 + \lambda_\sigma \left(|\sigma|^2 - \frac{v_{\text{PQ}}^2}{2} \right)^2 + \lambda_{H\sigma} \left(H^\dagger H - \frac{v^2}{2} \right) \left(|\sigma|^2 - \frac{v_{\text{PQ}}^2}{2} \right) \quad (2)$$

with v being the VEV of the SM Higgs H . After PQ symmetry breaking the first and the last terms in \mathcal{L}_Y give rise to

$$\begin{aligned} y \bar{Q}_L \sigma Q_R &\rightarrow \frac{y}{\sqrt{2}} \rho \bar{Q}_L Q_R e^{ia/f_a} + \frac{y}{\sqrt{2}} v_{\text{PQ}} \bar{Q}_L Q_R e^{ia/f_a} \\ \frac{1}{2} y_{ij} \bar{N}_{iR}^c \sigma N_{jR} &\rightarrow \frac{1}{2} \frac{y_{ij}}{\sqrt{2}} \rho \bar{N}_{iR}^c N_{jR} e^{ia/f_a} + \frac{1}{2} \frac{y_{ij}}{\sqrt{2}} v_{\text{PQ}} \bar{N}_{iR}^c N_{jR} e^{ia/f_a}. \end{aligned} \quad (3)$$

The phase part can be absorbed by the transformation $Q_R \rightarrow e^{-i\frac{a}{2f_a}} Q_R$ and $N_R \rightarrow e^{-i\frac{a}{2f_a}} N_R$. As the chiral transformation on Q is anomalous under QCD, this gives the term $\frac{g_s^2}{32\pi^2} \frac{a}{f_a} G_{\mu\nu} \tilde{G}^{\mu\nu}$ with $G_{\mu\nu}$ ($\tilde{G}^{\mu\nu}$) being (dual) field strength tensor of QCD. Simultaneously, from the kinetic term $\bar{Q} i \gamma^\mu \partial_\mu Q$, after transformation one gets the term $-\frac{\partial_\mu a}{2f_a} \bar{Q} \gamma^\mu \gamma_5 Q$. Similarly, from the kinetic term of RHN $\frac{i}{2} \bar{N} \gamma^\mu \partial_\mu N$, one gets the term $-\frac{1}{4} \frac{\partial_\mu a}{f_a} \bar{N} \gamma^\mu \gamma_5 N$. Now using the Dirac equation and the fact that the total derivative is zero at the boundary, we get

$$\begin{aligned} -\frac{\partial_\mu a}{2f_a} \bar{Q} \gamma^\mu \gamma_5 Q &= i \frac{M_Q}{f_a} a \bar{Q} \gamma_5 Q \\ -\frac{1}{4} \frac{\partial_\mu a}{f_a} \bar{N} \gamma^\mu \gamma_5 N &= \frac{i}{2} \frac{M_i}{f_a} a \bar{N} \gamma_5 N \end{aligned} \quad (4)$$

which define axion couplings to RHN and heavy quark Q . We have also dropped the chirality index from RHN notation and will denote them only by N_i with mass M_i hereafter.

III. AXION DARK MATTER, PBH, AND LEPTOGENESIS

We consider PBH to be formed in the early radiation-dominated Universe at a temperature T_{in} , with an initial mass related to the particle horizon size as [50, 79]

$$m_{\text{in}} = \frac{4}{3} \pi \gamma \left(\frac{1}{\mathcal{H}(T_{\text{in}})} \right)^3 \rho_{\text{R}}(T_{\text{in}}) \quad (5)$$

with ρ_{R} , \mathcal{H} indicating the radiation energy density and the Hubble parameter respectively. $\gamma \simeq 0.2$ is a numerical factor that contains the uncertainty of the PBH formation. The initial abundance of PBH during their formation is denoted by

$$\beta = \frac{\rho_{\text{PBH}}(T_{\text{in}})}{\rho_{\text{R}}(T_{\text{in}})}, \quad (6)$$

where ρ_{PBH} represents the PBH energy density. After their production, PBH evolve as matter and dominate the energy density of the early Universe, if their initial fractional energy density is greater than a critical value given by

$$\beta \geq \beta_{\text{crit}} \simeq 2.5 \times 10^{-14} \gamma^{-\frac{1}{2}} \left(\frac{m_{\text{in}}}{10^8 \text{g}} \right)^{-1}. \quad (7)$$

Finally, PBH lose their mass through Hawking radiation and completely evaporate at a temperature

$$T_{\text{ev}} \simeq \left(\frac{9g_{*,B}(T_{\text{BH}})}{10240} \right)^{\frac{1}{4}} \left(\frac{M_{\text{P}}^5}{m_{\text{in}}^3} \right)^{\frac{1}{2}}, \quad (8)$$

where M_{P} is the reduced Planck mass and $g_{*,B}(T_{\text{BH}}) \simeq 100$ being the relativistic degrees of freedom below T_{BH} . For QCD axions, the zero temperature mass ($T \leq T_{\text{QCD}} \simeq 150$ MeV) is related to PQ symmetry breaking scale, f_a as

$$m_a \simeq 5.7 \left(\frac{10^{12} \text{ GeV}}{f_a} \right) \mu\text{eV}. \quad (9)$$

Above $T > T_{\text{QCD}}$, the temperature-dependent axion mass is given as

$$m_a(T) = m_a \left(\frac{T_{\text{QCD}}}{T} \right)^4. \quad (10)$$

As indicated by lattice simulation, the power of 4 is not precise [78], but it does not affect our overall results significantly. If the PQ symmetry breaks in post inflationary era, the initial misalignment angle, $\theta_i = a_i/f_a$ takes the average value $\theta_i = \frac{\pi}{\sqrt{3}} \sim 1.81$. At high

temperatures, the axion evolution is friction-dominated and frozen at θ_i . It then starts to oscillate at a temperature T_{osc} , when the Hubble rate becomes comparable to axion mass: $\mathcal{H}(T_{\text{osc}}) \sim 3m_a(T_{\text{osc}})$. From the onset of oscillations temperature, axion starts behaving as matter, and from conservation of comoving number density, its number density at a later epoch can be written as

$$n_a(T) = n_a(T_{\text{osc}}) \frac{s(T)}{s(T_{\text{osc}})}, \quad (11)$$

where $s(T)$ is the comoving entropy density at a temperature T . The axion behaves as cold matter and can make all the observed dark matter abundance with total abundance

$$\Omega_a h^2 = \frac{\rho_a(T_0)}{\rho_c} h^2 = \frac{m_a(T_0)}{\rho_c} \left(\frac{\rho_a(T_{\text{osc}})}{m_a(T_{\text{osc}})} \frac{s(T)}{s(T_{\text{osc}})} \right) h^2. \quad (12)$$

Here ρ_c represents the critical energy density of the Universe today. If axion constitutes all the dark matter, it should have a mass around $\sim 14 \mu\text{eV}$, when produced via the misalignment mechanism [78]. The presence of PBH modifies the axion dark matter abundance in two different ways: (1) PBH change the oscillation temperature T_{osc} , because ρ_{PBH} contributes to Hubble expansion rate \mathcal{H} ; (2) PBH evaporation dilutes the existing abundance of axions via entropy injection. The latter effect is the dominant one. In addition to affecting the axion dark matter abundance, PBH evaporation can also produce axions. However, these axions behave as dark radiation contributing to N_{eff} . We numerically study the evolution of the PBH-axion system, closely following Ref. [40] (see Appendix A).

Lepton asymmetry can be generated thermally (with the thermal production of RHNs mediated by Yukawa couplings) at a high scale via the CP-violating decays of RHNs, which can be converted to the baryon asymmetry through the electroweak sphaleron processes [16]. At a temperature $T \sim M_i$, lepton asymmetry produced by i th RHN freezes out; therefore, M_i is typically the scale of thermal leptogenesis; $M_i \equiv \Lambda_{\text{lepto}}$. In the high-scale leptogenesis scenario, there are three distinct regimes of leptogenesis. The RHNs produce lepton doublets as a coherent superposition of flavors: $|L_i\rangle = A_{i\alpha} |L_{\alpha i}\rangle$, where $\alpha = e, \mu, \tau$ and $A_{i\alpha}$ is the corresponding amplitude determined by $F_{i\alpha}$. For temperatures $T \gtrsim 10^{12}$ GeV, all the charged lepton Yukawa couplings are out of equilibrium (the interaction strength is given by $\Gamma_\alpha \sim 5 \times 10^{-3} T h_\alpha$, with h_α being the charged lepton Yukawa coupling) and do not participate in the leptogenesis process. This is the unflavor or the vanilla regime of leptogenesis. In this regime, leptogenesis is not sensitive to the neutrino mixing matrix, e.g., mixing angles

and low-energy CP phases [80]. When the temperature drops down to $T \lesssim 10^{12}$ GeV, the τ flavored charged lepton interaction comes into equilibrium and breaks the coherent $|L_i\rangle$ state into τ and a composition of $e + \mu$ flavor (two flavor regime). Likewise, the later composition is broken once $T \lesssim 10^9$ GeV, when the μ flavored charged lepton interaction comes into equilibrium (three flavor regime). In both these flavored regimes, leptogenesis may be sensitive to the low-energy neutrino parameters because the neutrino mixing matrix cannot be eliminated from the CP asymmetry parameter. Therefore, for $T \sim M_i \gtrsim 10^{12}$ GeV, practically there are no ways to test high-scale thermal leptogenesis, barring some recent effort with gravitational waves from topological defects [24–28]. As mentioned in the introduction, here we show, in the unified setup of axion and seesaw, the vanilla regime is testable with axion physics as well as gravitational waves from PBH density fluctuations.

A crucial aspect of this work is to obtain the correct DM density for large $f_a \gtrsim 10^{12}$ GeV, requiring PBH evaporation after axion oscillation so that the overdensity of DM can be diluted. As we shall see, the required range of PBH mass for this does not affect the lepton asymmetry production (happens around $T \sim f_a$), however, dilutes it similarly to the DM density, and therefore correlates both of them.

For hierarchical RHNs, the CP asymmetry parameter can be estimated as [81, 82]

$$\epsilon_1 = \frac{3M_1 \sqrt{(\Delta m_{\text{atm}})^2}}{4\pi v^2}, \quad (13)$$

with $v/\sqrt{2} = 174$ GeV is the VEV of the SM Higgs and $(\Delta m_{\text{atm}})^2 \simeq 2.4 \times 10^{-3} \text{eV}^2$ is the active neutrino atmospheric mass-squared difference. The resulting baryon asymmetry from the decay of N_1 can be approximately written in terms of baryon-to-photon ratio as [83]

$$\eta_B \approx 10^{-2} \kappa_1 \frac{\epsilon_1}{\xi}. \quad (14)$$

Here ξ denotes the entropy dilution due to PBH evaporation, estimated as [83]

$$\xi = 233 \beta \left(\frac{m_{\text{in}}}{M_{\text{Pl}}} \right) \left(\frac{\gamma}{g_{*,B}(T_{\text{BH}}) \mathcal{G}} \right)^{1/2}, \quad (15)$$

and $\kappa_1 \simeq 10^{-2}$ is the efficiency of lepton asymmetry production. $\mathcal{G} \sim 3.8$ is the greybody factor and $M_{\text{Pl}} = \sqrt{8\pi} M_{\text{P}}$ is the Planck mass. The extra factor 10^{-2} on the right-hand side of Eq.(14) accounts for the combined effects of sphaleron conversion of the leptons to baryons

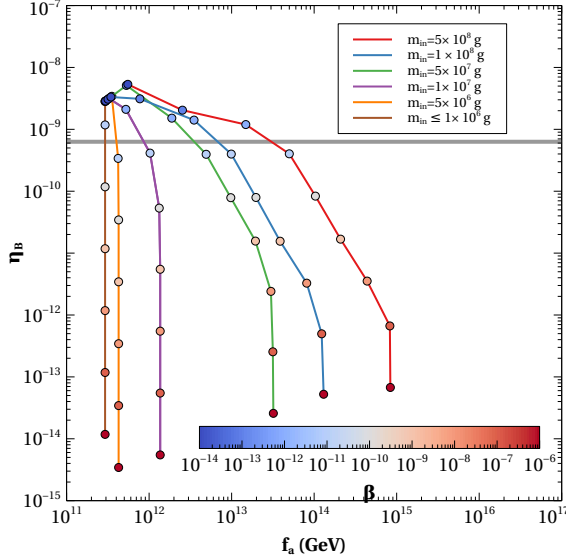


FIG. 2: Baryon to photon ratio, η_B versus f_a for different PBH mass and initial fractional abundance, β . Here, the contours satisfy the correct DM relic. Initial misalignment angle is taken to be $\theta_i = \frac{\pi}{\sqrt{3}} \sim 1.81$. The horizontal gray line denotes the observed value of η_B . Here, we consider $M_1 = f_a$ which gives us Eq.(16).

plus the photon dilution [81]. Because of our proposed unification $f_a \simeq M_1$,⁴ Eq.(13), (14), and (15) impose the following condition on β :

$$\beta \simeq 5.7 \times 10^{-12} \left(\frac{M_{\text{Pl}}}{m_{\text{in}}} \right) \frac{f_a}{\text{GeV}} \simeq 32.3 \left(\frac{M_{\text{Pl}}}{m_{\text{in}}} \right) \left(\frac{1 \mu\text{eV}}{m_a} \right). \quad (16)$$

Eq.(16) is the most important analytical relation we derive. Because of this stringent relation among β , m_{in} , and $f_a(m_a)$, concurrent generation of correct DM and BAU occurs for an extremely constrained parameter space as analyzed below in detail.

In Fig.2, we show the baryon asymmetry as a function of the PQ scale f_a , for different values of initial PBH mass. The contours shown are consistent with the observed DM relic from axion oscillation. If PBH evaporates before the axion oscillation temperature T_{osc} , they do not affect the axion dynamics. For $m_{\text{in}} \lesssim 10^6$ g, the PBH evaporation temperature remains higher than T_{osc} leading to the standard axion results with $f_a \simeq 3 \times 10^{11}$ GeV, generating the correct DM relic. This is indicated by the left-most brown-colored contour

⁴ Note that here we use the formula for the CP asymmetry parameter valid only for a hierarchical mass spectrum of RHNs, and we consider a N_1 -dominated leptogenesis scenario. In this case, although the heavier RHNs do not have any significant role to play, their masses are constrained as $M_{i=2,3} < f_a \sqrt{4\pi}$.

in Fig.2. Along this contour, β is varied, as per the color bar, which changes the baryon asymmetry because of entropy dilution, following Eq.(15). Increasing the PBH mass above 10^6 g decreases the oscillation temperature and reduces axion abundance because of entropy dilution, resulting in a higher f_a to obtain the observed DM abundance. With a decrease in β , this cumulative effect of PBH starts to diminish and hence the contours move towards the standard case of $f_a \simeq 3 \times 10^{11}$ GeV.

On the other hand, decreasing f_a and β has opposite effects on the baryon asymmetry η_B , with the former decreasing the asymmetry by decreasing M_1 (cf. Eq.(13)), while the latter increasing the asymmetry because of lesser entropy dilution. The latter effect turns out to be more dominant, leading to an increase in the value of η_B .

The lepton asymmetry can be significantly enhanced if two of the RHNs are quasi-degenerate, i.e., $\Delta M = M_2 - M_1 \ll \bar{M} = (M_1 + M_2)/2$ leading to the resonant leptogenesis scenario [84, 85]. For $\Delta M \simeq \Gamma$, the CP asymmetry parameter can reach up to $\mathcal{O}(1)$, where Γ indicates the decay width of the RHN. For the resonant scenario, the expression for β can be derived as

$$\beta = 2.9 \times 10^4 \epsilon_1 \left(\frac{M_{\text{Pl}}}{m_{\text{in}}} \right). \quad (17)$$

We quantify the results for both, the hierarchical and the resonant leptogenesis scenarios on the $m_{\text{in}} - \beta$ plane in Fig.3. The variation of axion mass is represented by the color gradient (see also the contours). For PBH mass $m_{\text{in}} \lesssim 10^{6.5}$ g, the evaporation of PBH occurs before the onset of axion oscillation, thereby not changing the axion abundance. Similarly, in the radiation domination region (below the blue line), PBH do not affect the axion abundance. For $m_{\text{in}} \gtrsim 10^{6.5}$ g, PBH delay the oscillation temperature plus dilute the axion density. Therefore, an ample amount of axions is required before PBH evaporation so that the correct DM relic is satisfied. This is achieved by reducing the axion mass (or increasing the PQ symmetry breaking scale f_a). The larger the m_{in} , the stronger the entropy production and therefore smaller the axion mass (larger f_a).

The observed baryon asymmetry constraints for the hierarchical (left) and resonant scenario (right) are shown with the red curves. For the PBH mass range, $10^{5.5}\text{g} \lesssim m_{\text{in}} \lesssim 10^{6.5}\text{g}$, the CP asymmetry parameter remains constant as $M_1 \sim f_a \sim 10^{11}$ as the axion DM production is not affected by PBH. Therefore, for a fixed f_a , the correlation between β and m_{in} determined according to Eq.(16) (β decreases with the increase of m_{in}). For $m_{\text{in}} \gtrsim 10^{6.5}$

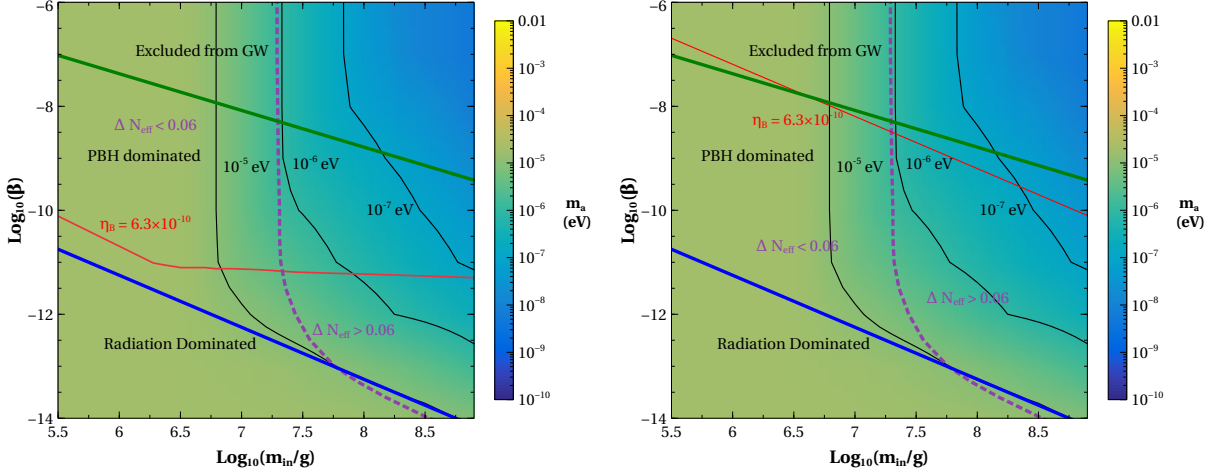


FIG. 3: Constraint on m_{in} versus β plane considering a hierarchical N_1 -dominated leptogenesis scenario (left plot) and a resonant leptogenesis scenario (right plot). The color bar represents the axion mass that satisfies the observed DM abundance. The red color lines in both plots denote the parameter space that is consistent with both, DM relic and baryon asymmetry. The region excluded from GW is separated by the solid green line. The magenta dashed line separates the regions that can be probed by future CMB-S4 experiments due to the contribution of hot axion on N_{eff} .

g, an increase in PBH mass increases the axion scale f_a owing to the interplay of entropy dilution and producing correct DM abundance. Because the CP asymmetry increases monotonically with f_a , in this case, a sharp decrease in β with the increase of m_{in} gets partially compensated, resulting in a plateau in the red curve (left). The region below (above) the red curve corresponds to $\eta_B > (<) 6.3 \times 10^{-10}$. As we shall discuss in sec.IV, the allowed values of β in this hierarchical leptogenesis scenario produce GWs with weaker amplitude (the maximum value of β allowed by N_{eff} constraint on GWs is shown with the green line) compared to its resonant version.

In the right panel of Fig.3, we show the results for the resonant leptogenesis scenario. Instead of Eq.(13), here we have considered a maximal CP asymmetry $\epsilon_1 = 0.1$, achievable with resonant enhancement. Due to this enhancement in the value CP asymmetry parameter value, strong entropy dilution and therefore for a given PBH mass, a larger value of β is required to produce the observed BAU. This is evident from the upward shift of the solid red line compared to the one in the left panel. In addition, due to a larger value of β , the

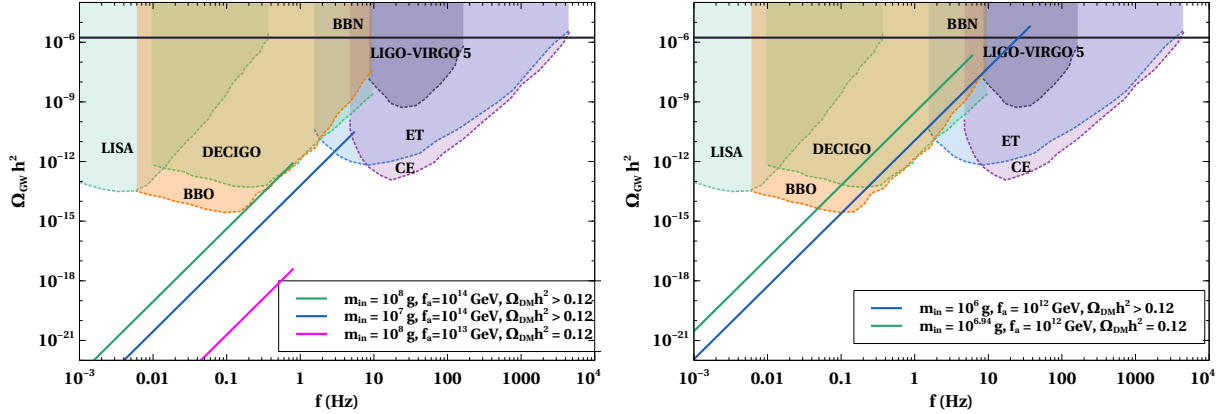


FIG. 4: Left panel: GW spectrum for hierarchical scenario. Right panel: GW spectrum for the resonant scenario.

resonant leptogenesis scenario produces much stronger GWs compared to the hierarchical case.

For completeness, in both the plots, we also indicate the parameter space within reach future CMB experiments like CMB-S4 [86] which can measure additional relativistic degrees of freedom ΔN_{eff} . Such non-zero ΔN_{eff} or dark radiation arises in our setup due to the production of hot axions from PBH evaporation. Note remarkably that in both the plots, the $T \sim M_i \sim f_a \gtrsim 10^{12}$ GeV is potentially testable, with either axion detectors or in combination with GW experiments.

IV. DETECTION PROSPECTS

A. Signatures in the form of GW from PBH density fluctuation

Recently it has been pointed out that GWs arise from the inhomogeneities in the PBH distribution after they are formed [34–38]. This particular source of GW is generally independent of the PBH production mechanism. PBHs typically follow an inhomogeneous spatial distribution after formation obeying Poisson statistics [34]. Such spatial inhomogeneities induce GW at second order once PBH dominate the energy density of the Universe [34, 35]. The amplitude of the GW gets further enhanced during PBH evaporation [35, 87].

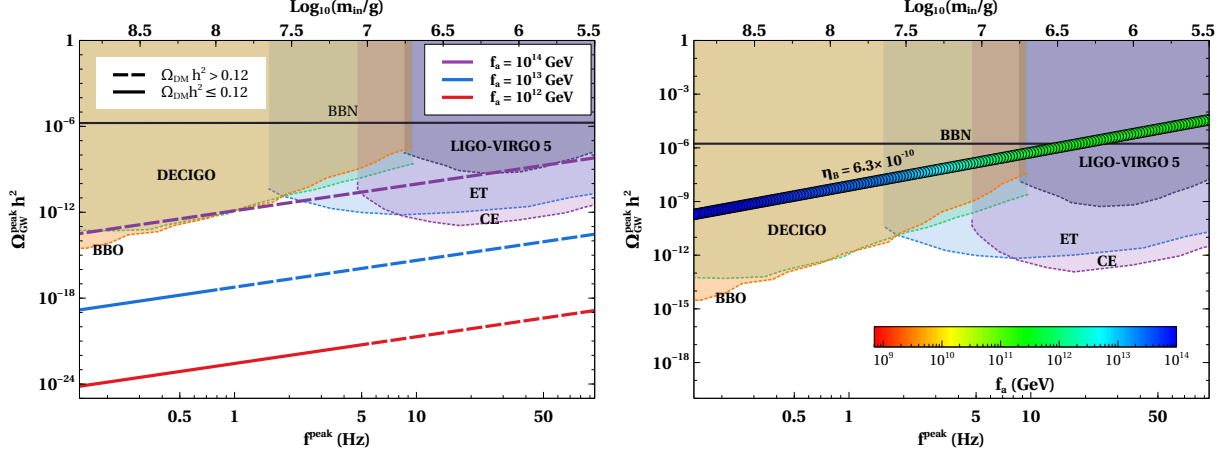


FIG. 5: Left panel: $\Omega_{\text{GW}}^{\text{peak}} h^2$ versus f^{peak} for hierarchical scenario with three different f_a . Right panel: $\Omega_{\text{GW}}^{\text{peak}} h^2$ versus f^{peak} for the resonant scenario with maximal CP asymmetry for correct axion DM abundance.

The amplitude of such GW is given by [35, 36, 55, 83]

$$\Omega_{\text{gw}}(t_0, f) \simeq \Omega_{\text{gw}}^{\text{peak}} \left(\frac{f}{f^{\text{peak}}} \right)^{11/3} \Theta(f^{\text{peak}} - f), \quad (18)$$

where $\Omega_{\text{gw}}^{\text{peak}}$ is the peak amplitude which depends on the initial PBH mass and energy fraction as

$$\Omega_{\text{gw}}^{\text{peak}} \simeq 2 \times 10^{-6} \left(\frac{\beta}{10^{-8}} \right)^{16/3} \left(\frac{m_{\text{in}}}{10^7 \text{g}} \right)^{34/9}. \quad (19)$$

On the other hand, the peak frequency f^{peak} which is related to the mean separation among PBH is given by

$$f^{\text{peak}} \simeq 1.7 \times 10^3 \text{ Hz} \left(\frac{m_{\text{in}}}{10^4 \text{g}} \right)^{-5/6}. \quad (20)$$

In order for the GW not to contradict the limits on N_{eff} from BBN and CMB observations, the following constraint on β must be satisfied

$$\beta \lesssim 1.1 \times 10^{-6} \left(\frac{m_{\text{in}}}{10^4 \text{g}} \right)^{-17/24}. \quad (21)$$

Note interestingly that Eq.(16), (17), and (19) relate leptogenesis scale and $\Omega_{\text{gw}}^{\text{peak}}$ by trading β , leading to the relation

$$\Omega_{\text{gw}}^{\text{peak}} \simeq 6.29 \times 10^{-22} \left(\frac{f_a}{10^{12} \text{GeV}} \right)^{16/3} \left(\frac{10^7 \text{g}}{m_{\text{in}}} \right)^{14/9} \quad (22)$$

for hierarchical leptogenesis, and

$$\Omega_{\text{gw}}^{\text{peak}} \simeq 1.71 \times 10^{-7} \left(\frac{\epsilon_1}{0.1} \right)^{16/3} \left(\frac{10^7 \text{g}}{m_{\text{in}}} \right)^{14/9} \quad (23)$$

for resonant leptogenesis, where for the latter scenario ϵ_1 is expressed as a function of f_a and mass splitting $\sim (M_2 - M_1)M_2^{-1}$ between two degenerate RHNs. To relate GW with a successful co genesis, Eq.(22) and (23) are required to be analysed with the constraint from correct axion DM production. Similar to the previous section, this has been implemented by solving the set of Boltzmann equations for axion and PBH (cf. AppendixA).

In Fig.4, we show the GW spectra for the hierarchical (left panel) and the resonant scenario (right panel), along with the sensitivity of different GW experiments such as advanced LIGO-VIRGO/LIGO 5 [88], LISA [89], DECIGO [90] and CE [91]. The spectra are plotted using Eq.(18) along with Eq.(22) and (23). The corresponding $\{m_{\text{in}}, f_a\}$ values are marked in the legend. Each spectrum corresponds to a different DM relic density but is consistent with the observed baryon asymmetry. Note that the signal strength is relatively weaker for the hierarchical leptogenesis case (left panel) when the model produces the correct DM relic (the magenta) curve. We however would like to mention that future planned detectors such as UDECIGO (UDECIGO-corr) [92, 93] can test such signal. On the other hand, for the resonant case, one obtains much stronger signal strength (right) without overproducing the DM. The reason being, as discussed in the previous section, resonant leptogenesis scenario requires a large value of β , and the peak amplitude goes as $\Omega_{\text{gw}}^{\text{peak}} \sim \beta^{16/3}$, see Eq.(19).

Plots in Fig.5, represent an enlarged parameter space covering $\Omega_{\text{GW}}^{\text{peak}} h^2$ and f^{peak} for a wide range of m_{in} . The left panel plot represents the hierarchical leptogenesis leading to successful BAU. The solid (dashed) segment in the curves represents the correct (overproduced) DM abundance. As discussed earlier, because resonant cases allow strong amplitude GW, we find it sufficient to show the GW spectra only for correct DM abundance (right panel).

Note also that, although arguable [94], one can potentially have GWs from axion-strings [95] in this model. Due to the PBH domination, our scenario can marginally access the values $f_a \gtrsim 10^{14}$ GeV to produce GWs from axion cosmic strings. However, we do not discuss this spectrum because, in the presence of PBH, a string-PBH network evolution requires numerical simulation [96].

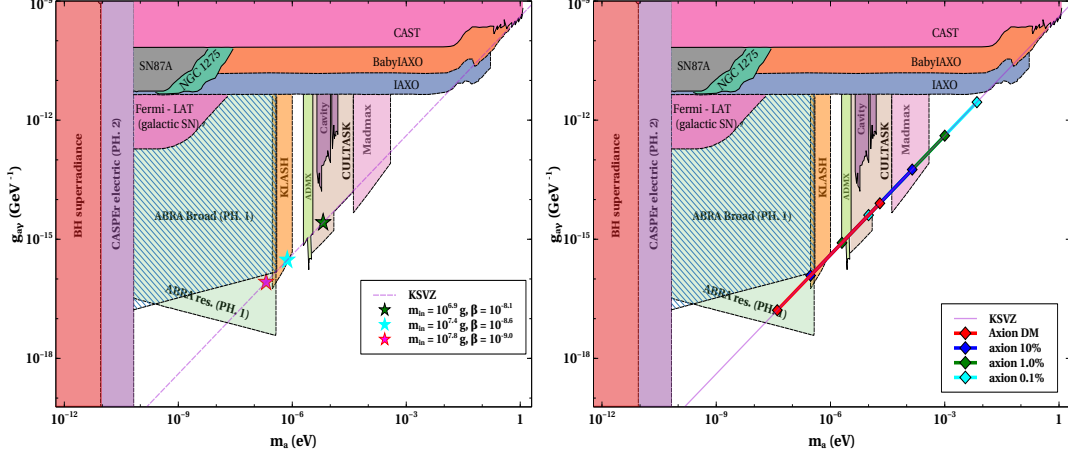


FIG. 6: Left panel: Axion-photon coupling versus axion mass in presence of PBH for three different sets of $\{m_{\text{in}}, \beta\}$ denoted by green, cyan, and magenta colored star-shaped points. Cogenesis with resonant leptogenesis is possible for all three points. Also, all three sets of $\{m_{\text{in}}, \beta\}$ come within future GW experiments (see related text for more details). Right panel: Constraints on axion-photon coupling in the presence of PBH for four different axion contributions to DM.

B. Signatures on $g_{a\gamma} - m_a$ plane

The axion detection prospects in most experiments primarily rely on axion-photon coupling. The axion-photon coupling leading to $\frac{1}{4}g_{a\gamma}aF\tilde{F}$ is given by (same as KSVZ model) [97]

$$g_{a\gamma} = -\frac{\alpha}{2\pi f_a} \left(\frac{2}{3} \frac{4m_d + m_u}{m_u + m_d} \right) = -1.92 \frac{\alpha}{2\pi f_a}, \quad (24)$$

with α being the fine-structure constant. Fig.6 shows the axion-photon coupling with axion mass including the bounds and sensitivities of different experiments. The current experimental bound on the axion-photon coupling from various experiments or observables are shown by the solid color lines (CAST [98, 99], SN87A [100–102], NGC 1275 [103], ADMX [104–106]) whereas future experimental sensitivities are shown by the dashed lines (CASPER [107], KLASH [108–110], ABRACADABRA [111, 112], CULTASK [113, 114], MADMAX [115], IAXO [116, 117], Fermi-LAT [118], BH superradiance [119]).

The left panel of Fig.6 shows the constraints on $g_{a\gamma}$ in the presence of PBH for three different axion mass associated with three different sets of $\{m_{\text{in}}, \beta\}$. These three points are indicated by green, cyan, and magenta colored star-shaped point (\star). For all three points, both DM relic and correct baryon asymmetry (with resonant leptogenesis) are satisfied.

While the green point comes within the sensitivity of future CULTASK experiment, the cyan and magenta points can be probed by future KLASH and ABRACADABRA experiments. Apart from their signatures in axion detection experiments, the three sets of $\{m_{\text{in}}, \beta\}$ also lie within the sensitivity of future DECIGO. This provides a complementary probe ofogenesis in terms of GWs and axion detection experiments. Note that for a smaller value of β (cf. left panel of Fig.3), the scenario of hierarchical leptogenesis can also be within the sensitivity of axion experiments, however with a weaker GW signal.

We conclude with the following remark: Because we consider axions to constitute the entire DM density, the overall scenario is highly constrained. This framework, however, can naturally allow one of the RHNs to make up the dominant dark matter density while keeping axion abundance subdominant. In which case, the predictions of this scenario would be very different. Interested readers may look up to a detailed discussion presented on this in Appendix B, C, and D. Here for example, in the right panel of Fig.6, we show the constraint for four different situations where axion contribution to DM is 100%, 10%, 1% and 0.1% denoted by red, blue, green, and cyan line respectively. The minimum f_a is obtained for PBH mass with $T_{\text{ev}} > T_{\text{osc}}$ (i.e. $m_{\text{in}} \lesssim 10^{6.5} \text{g}$). The maximum f_a is obtained for PBH mass with $T_{\text{ev}} \sim T_{\text{BBN}}$ and for maximum allowed β from Eq.(21) (i.e. $m_{\text{in}} \sim 10^{8.6} \text{g}$ and $\beta \sim 6 \times 10^{-10}$). While in this scenario the vanilla leptogenesis parameter space is still accessible, a striking difference would be to have only resonant leptogenesis for successful baryogenesis.

V. CONCLUSION

The presence of an early matter-dominated epoch in the early Universe allows a larger axion decay constant f_a consistent with correct DM abundance. We implement this idea in a SMASH-like setup where the f_a and seesaw or leptogenesis scale are equivalent. We show that contrary to the EMD provided, e.g., by a long-lived field, a PBH-domination scenario is markedly testable with gravitational waves alongside the axion experiments that intend to detect low-mass axions ($m_a \lesssim 10^{-5} \text{eV}$). In particular, this setup opens up a novel opportunity to test unflavored leptogenesis scales $f_a \gtrsim 10^{12} \text{GeV}$, which are otherwise neither testable from measurements of neutrino mixing parameters like Dirac CP phase nor accessible directly at terrestrial experiments. A hierarchical (resonant) leptogenesis scenario produces weaker (stronger) gravitational waves within the frequency band of planned GW

detectors. A successfulogenesis renders extremely constrained model parameter space and thereby robust predictions. In addition to GW and axion detection prospects, we can also have observable dark radiation in future CMB experiments due to the axions produced from PBH evaporation. This keeps our cogenesis setup verifiable at gravitational wave, axion detectors as well as CMB experiments.

Acknowledgements

We thank Satyabrata Datta for the discussion at the initial stages of this work. The work of DB is supported by the Science and Engineering Research Board (SERB), Government of India grants MTR/2022/000575 and CRG/2022/000603. The work of ND is supported by the Ministry of Education, Government of India via the Prime Minister's Research Fellowship (PMRF) December 2021 scheme. ND would like to thank Disha Bandyopadhyay for useful discussions. The work of SJD was supported by IBS under the project code, IBS-R018-D1. SJD would also like to thank the support and hospitality of the Tata Institute of Fundamental Research (TIFR), Mumbai, where a part of this project was carried out.

Appendix A: Axion field evolution

PBH, after formation, loses its energy via Hawking evaporation. The combined Boltzmann equations for the system can be written as

$$\frac{d\rho_{\text{in}}}{dt} + 3\mathcal{H}\rho_{\text{BH}} = \frac{1}{m_{\text{BH}}} \frac{dm_{\text{BH}}}{dt} \rho_{\text{BH}} \quad (\text{A1})$$

$$\frac{d\rho_r}{dt} + 4\mathcal{H}\rho_r = -\frac{1}{m_{\text{in}}} \frac{dm_{\text{BH}}}{dt} \rho_{\text{BH}}. \quad (\text{A2})$$

The PBH mass loss rate is given by

$$\frac{1}{m_{\text{BH}}} \frac{dm_{\text{BH}}}{dt} = -\frac{\mathcal{G}g_H(T_H)}{30720\pi G^2 m_{\text{BH}}^3}. \quad (\text{A3})$$

Due to PBH evaporation, entropy injection takes place, leading to non-conservation of entropy. The entropy injection can be tracked via

$$\frac{ds}{dt} + 3\mathcal{H}s = -\frac{1}{m_{\text{BH}}} \frac{dm_{\text{BH}}}{dt} \frac{\rho_{\text{BH}}}{T}. \quad (\text{A4})$$

The evolution of axion field a in the early Universe can be written as

$$\ddot{a} + 3\mathcal{H}\dot{a} + \frac{1}{R^2(t)}\nabla^2 a + \frac{\partial V(a, T)}{\partial a} = 0, \quad (\text{A5})$$

where

$$V(a, T) = f_a^2 m_a^2(T) \left(1 - \cos\left(\frac{a}{f_a}\right) \right) \quad (\text{A6})$$

and R denotes the scale factor. The initial axion angle, $\theta = \frac{a}{f_a}$ is frozen in until the oscillation temperature of axion which can be estimated by comparing Hubble expansion rate to the temperature dependent axion mass $\mathcal{H}(T_{\text{osc}}) = m_a(T_{\text{osc}})$. To get the contribution of axion to the current energy budget, we solve the above equations following the procedure in the reference [40]. The procedure is to first estimate the oscillation temperature T_{osc} in presence of PBH. With this, number density of axion at T_{osc} can be calculated following

$$n_a(T_{\text{osc}}) = \frac{\rho_a(T_{\text{osc}})}{m_a(T_{\text{osc}})} = \frac{1}{m_a(T_{\text{osc}})} \left(\frac{1}{2}\dot{a}^2 + \frac{1}{2}|\nabla a|^2 + V(a) \right). \quad (\text{A7})$$

Due to entropy dilution, the equation for n_a becomes

$$\frac{1}{n_a} \frac{d(n_a/s)}{dt} = \frac{1}{m_{\text{BH}}} \frac{dm_{\text{BH}}}{dt} \frac{\rho_{\text{BH}}}{Ts^2}. \quad (\text{A8})$$

The above equation is solved from $T \gtrsim T_{\text{osc}}$ to a sufficiently small temperature when PBH completely evaporates.

Appendix B: Multi-component Dark Matter

If axion does not constitute the entire DM, the allowed parameter space discussed so far can change significantly. The deficit in total DM abundance can be filled up by one of the RHNs, as discussed briefly in Appendix C. From the left panel of Fig.3, for a particular value of m_{in} and β , one needs a larger value of axion mass (correspondingly smaller value of f_a) to have sub-dominant axion DM. However, at the same time, a smaller value of f_a also reduces the CP asymmetry parameter according to Eq.(13). As a result, baryon asymmetry also reduces. Thus, for a particular PBH mass, one needs to consider a smaller value β so that dilution is also less to obtain correct baryon asymmetry. However, it turns out that for this particular scenario, even if one reduces β to β_c (where β_c distinguishes PBH-dominated and radiation-dominated region), the correct baryon asymmetry can not

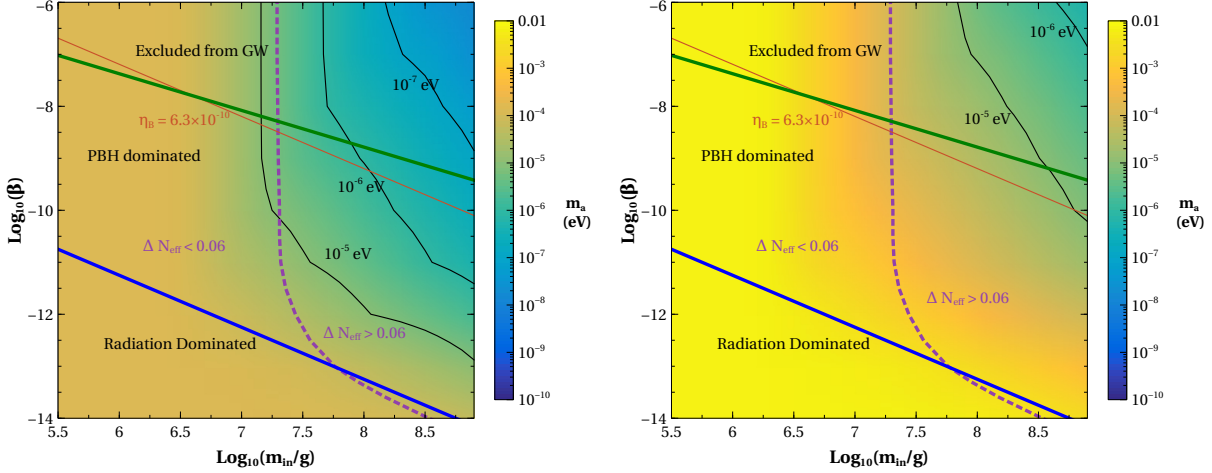


FIG. 7: Constraint on m_{in} versus β plane considering resonant leptogenesis. Axion constitutes 10%, 0.1% of total DM abundance in left and right panels respectively. The red solid lines in the plots denote the parameter space that is consistent with both DM relic and baryon asymmetry. The region excluded from GW is separated by solid green line. The magenta dashed line separate the regions that can be probed by future CMB-S4 experiment due to contribution of hot axion on N_{eff} .

be obtained. The maximum baryon asymmetry that can be obtained is $\sim 4 \times 10^{-10}$ which is less than the observed asymmetry, viz., 6.3×10^{-10} . All the region above the $\beta = \beta_c$ line gives $\eta_B < 4 \times 10^{-10}$. For the sub-dominant axion DM scenario, one therefore must consider the resonant leptogenesis approach to generate the correct BAU. In Fig.7 we show the results for resonant leptogenesis by considering the percentage of axion DM as a free parameter. The solid red line in these plots correspond to the parameter space consistent with observed baryon asymmetry for $\epsilon_1 = 0.1$.

Note that, in the multi-component DM scenario, because the axion DM is a subdominant component, we can have smaller f_a values leading to axion mass range in the solar axion ballpark [117, 120], making this scenario pretty different from the case of axion constituting 100% DM. As an aside, let us mention that there have been efforts to obtain the entire dark matter relic only in the form of axions for a smaller value of decay constant ($f_a \sim 10^8 \text{ GeV}$) via parametric resonance production of axions. see. e.g., Refs.[121–123].

Appendix C: Production of Right-Handed Neutrino Dark Matter

As two RHNs are sufficient to generate neutrino mass and BAU via leptogenesis, the other RHN, if sufficiently long-lived, can constitute some part of the total DM abundance. Due to the presence of PBH and RHN coupling to axion as well as SM leptons, we can have three⁵ different production channels for RHN DM namely, (i) gravitational production from PBH evaporation [41–58], (ii) production via axion portal interactions [126–128], (iii) freeze-in production via Yukawa portal interactions [129, 130].

For the axion decay constant we have in our setup, superheavy RHN DM is more natural which is produced dominantly via PBH evaporation. For the case when $M_{\text{DM}} < T_{\text{BH}}^{\text{in}}$, correct relic abundance needs DM mass in the range of $\sim \text{GeV}$. However, for this mass range of DM produced by PBH evaporation, the DM turns out to be hot and hence disfavored from structure formation constraints. For the other limiting case $M_{\text{DM}} > T_{\text{BH}}^{\text{in}}$, the DM mass is greater than 10^9 GeV , keeping it in the superheavy ballpark, a natural consequence of the high PQ symmetry breaking scale

However, if we allow fine-tuning of RHN DM mass, keeping it much lower than the PQ scale, other production mechanisms like axion portal can dominate. Since, axion portal coupling of RHN will be suppressed for allowed mass range of thermal DM below unitarity limit [131], such production is likely to occur via freeze-in mechanism from the SM bath. For $f_a \sim 10^{12} \text{ GeV}$ and reheat temperature $T_{\text{RH}} \sim 10^{12} \text{ GeV}$, we require DM mass to be around 10^5 GeV for observed DM relic to be produced via UV freeze-in. For heavier DM mass, it is likely to be overproduced via axion portal interactions as long as $T_{\text{RH}} > M_{\text{DM}}$. On the other hand, RHN DM of mass $\sim 10^5 \text{ GeV}$ will also be overproduced from PBH evaporation as mentioned above. This pushes RHN DM to low mass where it can be produced efficiently via Yukawa portal interactions while gravitational and axion portal contributions remain sub-dominant. In this regime, correct relic can be achieved via IR freeze-in production of N_1 from the SM bath. As shown in earlier works [129, 130], such freeze-in production is dominated by W^\pm, Z and SM Higgs decays facilitated via active-sterile neutrino mixing θ_1 . The mixing angle can be tuned by choosing the lightest active neutrino mass m_1 . The same active-sterile mixing also leads to decay of N_1 into SM particles. Although the abundance

⁵ It is also possible to generate light RHN DM via active-sterile neutrino oscillation [124], though it faces severe X-ray constraints. See [125] for a review.

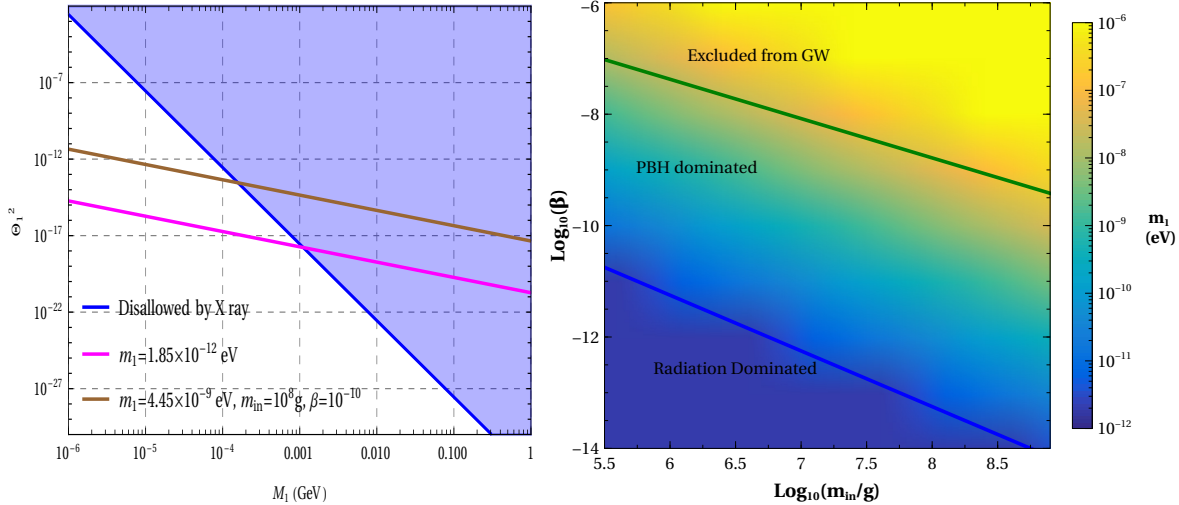


FIG. 8: Left panel: θ_1^2 versus M_1 for two different scenarios: without PBH and with PBH ($m_{in} = 10^8$ g and $\beta = 10^{-10}$) shown by magenta and brown color respectively. The shaded blue color region represents the excluded region by X-ray experiments. Right panel: Lightest neutrino mass m_1 in PBH parameter space $\beta - m_{in}$ with N_1 abundance $\Omega_{N_1} h^2 = 0.12$.

of N_1 only depends on m_1 , the decay rate of N_1 depends on both m_1 and M_1 . This gives a constraint on the N_1 mass, as shown in the left panel of Fig.8. The magenta-colored line represents the situation where PBH do not dominate the energy density of the Universe (i.e. no additional entropy dilution). The brown colored line denotes the situation where entropy dilution is present from PBH evaporation. Due to the presence of entropy dilution, N_1 should be produced over-abundantly requiring a larger value of active-sterile mixing angle. As the decay of N_1 is also dependent on θ_1^2 , so M_1 is more tightly constraint in the presence of entropy dilution as seen from the left plot of Fig.8. Here both the magenta and the brown color lines give the correct relic density. In the right panel plot, m_1 is shown in the $\beta - m_{in}$ plane for $\Omega_{N_1} h^2 = 0.12$, correlating neutrino mass with PBH parameters from correct DM relic criteria.

RHN DM with $T_{RH} < M_{DM}$: As noticed in the above discussions, the RHN DM parameter space produced from PBH evaporation and axion portal interactions is anti-correlated, forcing the RHN DM mass to sub-GeV ballpark where it can be efficiently produced from Yukawa portal freeze-in mechanisms. However, this requires severe fine-tuning of RHN coupling with the PQ scalar such that $M_1 \equiv M_{DM} \ll f_a$. Such unnatural fine-tuning can, however, be avoided if we consider the heaviest RHN N_3 to be DM with mass $M_3 = f_a > T_{RH}$

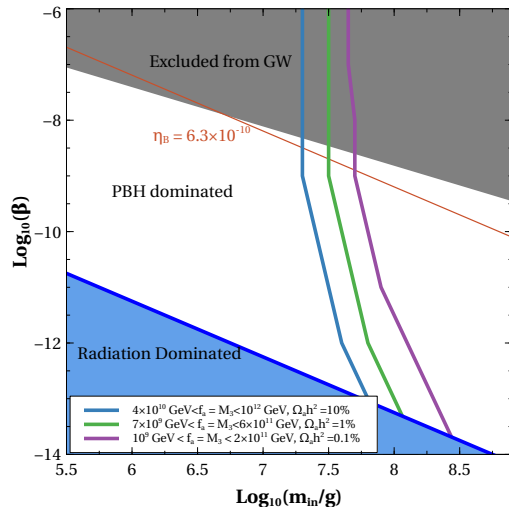


FIG. 9: For $M_3 \gg T_{\text{RH}} > M_2 \sim M_3$. Blue, green, and magenta colored lines denote the different situations where $\Omega_a h^2 = 10\%$, $\Omega_a h^2 = 1\%$ and $\Omega_a h^2 = 0.1\%$ respectively and $f_a = M_3$. The RHN N_3 constitutes the rest of DM abundance. The brown-colored solid line denotes the parameter space consistent with the baryon asymmetry for maximal CP asymmetry.

which can not be produced from the bath. Leptogenesis is obtained from N_1 and N_2 with $M_1 \simeq M_2$. For thermal leptogenesis, we assume $M_1 \simeq M_2 < T_{\text{RH}} \ll M_3 = f_a$. Although the PQ symmetry gets broken after e.g., slow-roll inflation, a non-instantaneous reheating phase [132] can lead to a reheat temperature $T_{\text{RH}} \ll f_a$. This leads to purely gravitational production of RHN DM from PBH evaporation. The DM mass produced from PBH evaporation is given by

$$M_{\text{DM}} \simeq 4.5 \times 10^3 \left(\frac{0.12}{\Omega_{N_3} h^2} \right) \left(\frac{m_{\text{in}}}{M_{\text{Pl}}} \right)^{-5/2} \frac{M_{\text{Pl}}^2}{\text{GeV}}. \quad (\text{C1})$$

Considering $M_{\text{DM}} = f_a$, this gives a line in the $\beta - m_{\text{in}}$ plane. In Fig.9, blue, green, and magenta colored lines correspond to the situations where $\Omega_a h^2 = 10\%$, 1% and 0.1% of total DM abundance respectively. Note that $M_3 = M_{\text{DM}} = f_a$ changes along these contours, following Eq.(C1). The rest of the DM abundance is constituted by N_3 . The observed BAU can be generated from resonant leptogenesis as discussed earlier. The parameter space satisfying the observed BAU for maximal CP asymmetry $\epsilon_1 = 0.1$ is indicated by the brown-colored solid line in Fig.9.

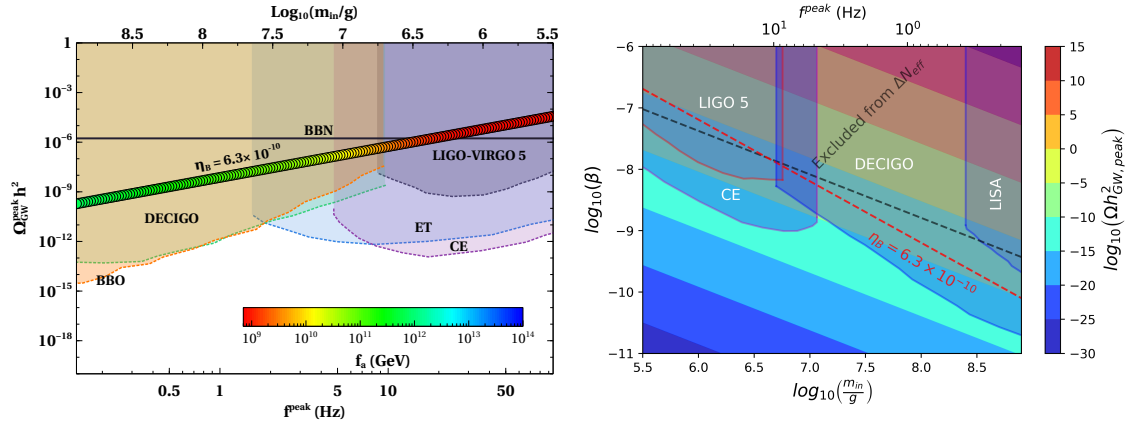


FIG. 10: Left panel: $\Omega_{\text{GW}}^{\text{peak}} h^2$ versus f^{peak} for 0.1% relative abundance of axion DM. Right Panel : Peak Gravitational Waves amplitude as a function of m_{in} and β with different experimental sensitivities. The red dashed line denotes the correct baryon asymmetry value for resonant leptogenesis with maximal CP asymmetry.

Appendix D: GW prospects in multi-component DM scenario

Similar to the right panel of Fig.5, we show the $\Omega_{\text{GW}}^{\text{peak}} h^2$ and f^{peak} for resonant leptogenesis scenario in the left panel of Fig.10 considering 0.1% relative abundance of axion DM. In the right panel, we show another representation of the resonant scenario where the peak GWs amplitude are shown as a function of PBH mass and β along with different GWs sensitivities. As expected, the red dashed colored line denoting correct leptogenesis for resonant scenario lies within the future GWs sensitivities.

-
- [1] C. Abel et al., *Measurement of the Permanent Electric Dipole Moment of the Neutron*, *Phys. Rev. Lett.* **124** (2020), no. 8 081803, [[arXiv:2001.11966](#)].
 - [2] R. D. Peccei and H. R. Quinn, *CP Conservation in the Presence of Instantons*, *Phys. Rev. Lett.* **38** (1977) 1440–1443.
 - [3] R. D. Peccei and H. R. Quinn, *Constraints Imposed by CP Conservation in the Presence of Instantons*, *Phys. Rev. D* **16** (1977) 1791–1797.
 - [4] F. Wilczek, *Problem of Strong P and T Invariance in the Presence of Instantons*, *Phys. Rev. Lett.* **40** (1978) 279–282.

- [5] S. Weinberg, *A New Light Boson?*, *Phys. Rev. Lett.* **40** (1978) 223–226.
- [6] J. Preskill, M. B. Wise, and F. Wilczek, *Cosmology of the Invisible Axion*, *Phys. Lett. B* **120** (1983) 127–132.
- [7] L. F. Abbott and P. Sikivie, *A Cosmological Bound on the Invisible Axion*, *Phys. Lett. B* **120** (1983) 133–136.
- [8] M. Dine and W. Fischler, *The Not So Harmless Axion*, *Phys. Lett. B* **120** (1983) 137–141.
- [9] G. G. Raffelt, *Astrophysical axion bounds*, *Lect. Notes Phys.* **741** (2008) 51–71, [[hep-ph/0611350](#)].
- [10] A. Caputo and G. Raffelt, *Astrophysical Axion Bounds: The 2024 Edition*, in *1st Training School of the COST Action COSMIC WISPerS (CA21106)*, 1, 2024. [arXiv:2401.13728](#).
- [11] M. Dine, W. Fischler, and M. Srednicki, *A Simple Solution to the Strong CP Problem with a Harmless Axion*, *Phys. Lett. B* **104** (1981) 199–202.
- [12] A. R. Zhitnitsky, *On Possible Suppression of the Axion Hadron Interactions. (In Russian)*, *Sov. J. Nucl. Phys.* **31** (1980) 260.
- [13] J. E. Kim, *Weak Interaction Singlet and Strong CP Invariance*, *Phys. Rev. Lett.* **43** (1979) 103.
- [14] M. A. Shifman, A. I. Vainshtein, and V. I. Zakharov, *Can Confinement Ensure Natural CP Invariance of Strong Interactions?*, *Nucl. Phys. B* **166** (1980) 493–506.
- [15] M. Kawasaki and K. Nakayama, *Axions: Theory and Cosmological Role*, *Ann. Rev. Nucl. Part. Sci.* **63** (2013) 69–95, [[arXiv:1301.1123](#)].
- [16] M. Fukugita and T. Yanagida, *Baryogenesis Without Grand Unification*, *Phys. Lett. B* **174** (1986) 45–47.
- [17] G. Servant, *Baryogenesis from Strong CP Violation and the QCD Axion*, *Phys. Rev. Lett.* **113** (2014), no. 17 171803, [[arXiv:1407.0030](#)].
- [18] S. Ipek and T. M. P. Tait, *Early Cosmological Period of QCD Confinement*, *Phys. Rev. Lett.* **122** (2019), no. 11 112001, [[arXiv:1811.00559](#)].
- [19] D. Croon, J. N. Howard, S. Ipek, and T. M. P. Tait, *QCD baryogenesis*, *Phys. Rev. D* **101** (2020), no. 5 055042, [[arXiv:1911.01432](#)].
- [20] R. T. Co and K. Harigaya, *Axiogenesis*, *Phys. Rev. Lett.* **124** (2020), no. 11 111602, [[arXiv:1910.02080](#)].
- [21] G. Ballesteros, J. Redondo, A. Ringwald, and C. Tamarit, *Standard*

- Model—axion—seesaw—Higgs portal inflation. Five problems of particle physics and cosmology solved in one stroke*, *JCAP* **08** (2017) 001, [[arXiv:1610.01639](#)].
- [22] J. D. Clarke and R. R. Volkas, *Technically natural nonsupersymmetric model of neutrino masses, baryogenesis, the strong CP problem, and dark matter*, *Phys. Rev. D* **93** (2016), no. 3 035001, [[arXiv:1509.07243](#)].
- [23] A. H. Sopov and R. R. Volkas, *VISHν: solving five Standard Model shortcomings with a Poincaré-protected electroweak scale*, *Phys. Dark Univ.* **42** (2023) 101381, [[arXiv:2206.11598](#)].
- [24] J. A. Dror, T. Hiramatsu, K. Kohri, H. Murayama, and G. White, *Testing the Seesaw Mechanism and Leptogenesis with Gravitational Waves*, *Phys. Rev. Lett.* **124** (2020), no. 4 041804, [[arXiv:1908.03227](#)].
- [25] S. Blasi, V. Brdar, and K. Schmitz, *Fingerprint of low-scale leptogenesis in the primordial gravitational-wave spectrum*, *Phys. Rev. Res.* **2** (2020), no. 4 043321, [[arXiv:2004.02889](#)].
- [26] B. Fornal and B. Shams Es Haghi, *Baryon and Lepton Number Violation from Gravitational Waves*, *Phys. Rev. D* **102** (2020), no. 11 115037, [[arXiv:2008.05111](#)].
- [27] R. Samanta and S. Datta, *Gravitational wave complementarity and impact of NANOGrav data on gravitational leptogenesis*, *JHEP* **05** (2021) 211, [[arXiv:2009.13452](#)].
- [28] B. Barman, D. Borah, A. Dasgupta, and A. Ghoshal, *Probing High Scale Dirac Leptogenesis via Gravitational Waves from Domain Walls*, [arXiv:2205.03422](#).
- [29] L. Visinelli and P. Gondolo, *Axion cold dark matter in non-standard cosmologies*, *Phys. Rev. D* **81** (2010) 063508, [[arXiv:0912.0015](#)].
- [30] A. E. Nelson and H. Xiao, *Axion Cosmology with Early Matter Domination*, *Phys. Rev. D* **98** (2018), no. 6 063516, [[arXiv:1807.07176](#)].
- [31] S. W. Hawking, *Black hole explosions*, *Nature* **248** (1974) 30–31.
- [32] S. W. Hawking, *Particle Creation by Black Holes*, *Commun. Math. Phys.* **43** (1975) 199–220. [Erratum: *Commun.Math.Phys.* 46, 206 (1976)].
- [33] B. Carr, K. Kohri, Y. Sendouda, and J. Yokoyama, *Constraints on primordial black holes*, *Rept. Prog. Phys.* **84** (2021), no. 11 116902, [[arXiv:2002.12778](#)].
- [34] T. Papanikolaou, V. Vennin, and D. Langlois, *Gravitational waves from a universe filled with primordial black holes*, *JCAP* **03** (2021) 053, [[arXiv:2010.11573](#)].
- [35] G. Domènech, C. Lin, and M. Sasaki, *Gravitational wave constraints on the primordial*

- black hole dominated early universe*, *JCAP* **04** (2021) 062, [[arXiv:2012.08151](#)]. [Erratum: *JCAP* **11**, E01 (2021)].
- [36] G. Domènech, V. Takhistov, and M. Sasaki, *Exploring evaporating primordial black holes with gravitational waves*, *Phys. Lett. B* **823** (2021) 136722, [[arXiv:2105.06816](#)].
- [37] G. Domènech, *Scalar Induced Gravitational Waves Review*, *Universe* **7** (2021), no. 11 398, [[arXiv:2109.01398](#)].
- [38] T. Papanikolaou, *Gravitational waves induced from primordial black hole fluctuations: the effect of an extended mass function*, *JCAP* **10** (2022) 089, [[arXiv:2207.11041](#)].
- [39] N. Bernal, F. Hajkarim, and Y. Xu, *Axion Dark Matter in the Time of Primordial Black Holes*, *Phys. Rev. D* **104** (2021) 075007, [[arXiv:2107.13575](#)].
- [40] K. Mazde and L. Visinelli, *The interplay between the dark matter axion and primordial black holes*, *JCAP* **01** (2023) 021, [[arXiv:2209.14307](#)].
- [41] P. Gondolo, P. Sandick, and B. Shams Es Haghi, *Effects of primordial black holes on dark matter models*, *Phys. Rev. D* **102** (2020), no. 9 095018, [[arXiv:2009.02424](#)].
- [42] N. Bernal and O. Zapata, *Dark Matter in the Time of Primordial Black Holes*, *JCAP* **03** (2021) 015, [[arXiv:2011.12306](#)].
- [43] A. M. Green, *Supersymmetry and primordial black hole abundance constraints*, *Phys. Rev. D* **60** (1999) 063516, [[astro-ph/9903484](#)].
- [44] M. Y. Khlopov, A. Barrau, and J. Grain, *Gravitino production by primordial black hole evaporation and constraints on the inhomogeneity of the early universe*, *Class. Quant. Grav.* **23** (2006) 1875–1882, [[astro-ph/0406621](#)].
- [45] D.-C. Dai, K. Freese, and D. Stojkovic, *Constraints on dark matter particles charged under a hidden gauge group from primordial black holes*, *JCAP* **06** (2009) 023, [[arXiv:0904.3331](#)].
- [46] R. Allahverdi, J. Dent, and J. Osinski, *Nonthermal production of dark matter from primordial black holes*, *Phys. Rev. D* **97** (2018), no. 5 055013, [[arXiv:1711.10511](#)].
- [47] O. Lennon, J. March-Russell, R. Petrossian-Byrne, and H. Tillim, *Black Hole Genesis of Dark Matter*, *JCAP* **04** (2018) 009, [[arXiv:1712.07664](#)].
- [48] D. Hooper, G. Krnjaic, and S. D. McDermott, *Dark Radiation and Superheavy Dark Matter from Black Hole Domination*, *JHEP* **08** (2019) 001, [[arXiv:1905.01301](#)].
- [49] P. Sandick, B. S. Es Haghi, and K. Sinha, *Asymmetric reheating by primordial black holes*, *Phys. Rev. D* **104** (2021), no. 8 083523, [[arXiv:2108.08329](#)].

- [50] T. Fujita, M. Kawasaki, K. Harigaya, and R. Matsuda, *Baryon asymmetry, dark matter, and density perturbation from primordial black holes*, *Phys. Rev. D* **89** (2014), no. 10 103501, [[arXiv:1401.1909](#)].
- [51] S. Datta, A. Ghosal, and R. Samanta, *Baryogenesis from ultralight primordial black holes and strong gravitational waves from cosmic strings*, *JCAP* **08** (2021) 021, [[arXiv:2012.14981](#)].
- [52] S. Jyoti Das, D. Mahanta, and D. Borah, *Low scale leptogenesis and dark matter in the presence of primordial black holes*, [arXiv:2104.14496](#).
- [53] B. Barman, D. Borah, S. J. Das, and R. Roshan, *Non-thermal origin of asymmetric dark matter from inflaton and primordial black holes*, *JCAP* **03** (2022), no. 03 031, [[arXiv:2111.08034](#)].
- [54] B. Barman, D. Borah, S. Das Jyoti, and R. Roshan, *Cogenesis of Baryon Asymmetry and Gravitational Dark Matter from PBH*, [arXiv:2204.10339](#).
- [55] B. Barman, D. Borah, S. Jyoti Das, and R. Roshan, *Gravitational wave signatures of a PBH-generated baryon-dark matter coincidence*, *Phys. Rev. D* **107** (2023), no. 9 095002, [[arXiv:2212.00052](#)].
- [56] A. Cheek, L. Heurtier, Y. F. Perez-Gonzalez, and J. Turner, *Primordial Black Hole Evaporation and Dark Matter Production: I. Solely Hawking radiation*, [arXiv:2107.00013](#).
- [57] A. Chaudhuri, B. Coleppa, and K. Loho, *Dark matter production from two evaporating PBH distributions*, *Phys. Rev. D* **108** (2023), no. 3 035040, [[arXiv:2301.08588](#)].
- [58] D. Borah, S. Jyoti Das, and I. Saha, *Dark matter from phase transition generated PBH evaporation with gravitational waves signatures*, [arXiv:2401.12282](#).
- [59] B. J. Carr, *Some cosmological consequences of primordial black-hole evaporations*, *Astrophys. J.* **206** (1976) 8–25.
- [60] D. Baumann, P. J. Steinhardt, and N. Turok, *Primordial Black Hole Baryogenesis*, [hep-th/0703250](#).
- [61] A. Hook, *Baryogenesis from Hawking Radiation*, *Phys. Rev. D* **90** (2014), no. 8 083535, [[arXiv:1404.0113](#)].
- [62] Y. Hamada and S. Iso, *Baryon asymmetry from primordial black holes*, *PTEP* **2017** (2017), no. 3 033B02, [[arXiv:1610.02586](#)].
- [63] L. Morrison, S. Profumo, and Y. Yu, *Melanopogenesis: Dark Matter of (almost) any Mass*

- and Baryonic Matter from the Evaporation of Primordial Black Holes weighing a Ton (or less), *JCAP* **05** (2019) 005, [[arXiv:1812.10606](#)].
- [64] D. Hooper and G. Krnjaic, *GUT Baryogenesis With Primordial Black Holes*, *Phys. Rev. D* **103** (2021), no. 4 043504, [[arXiv:2010.01134](#)].
- [65] Y. F. Perez-Gonzalez and J. Turner, *Assessing the tension between a black hole dominated early universe and leptogenesis*, [arXiv:2010.03565](#).
- [66] N. Smyth, L. Santos-Olmsted, and S. Profumo, *Gravitational Baryogenesis and Dark Matter from Light Black Holes*, [arXiv:2110.14660](#).
- [67] N. Bernal, C. S. Fong, Y. F. Perez-Gonzalez, and J. Turner, *Rescuing High-Scale Leptogenesis using Primordial Black Holes*, [arXiv:2203.08823](#).
- [68] A. Ambrosone, R. Calabrese, D. F. G. Fiorillo, G. Miele, and S. Morisi, *Towards baryogenesis via absorption from primordial black holes*, *Phys. Rev. D* **105** (2022), no. 4 045001, [[arXiv:2106.11980](#)].
- [69] G. Franciolini, *Primordial Black Holes: from Theory to Gravitational Wave Observations*. PhD thesis, Geneva U., Dept. Theor. Phys., 2021. [arXiv:2110.06815](#).
- [70] C.-M. Yoo, *The Basics of Primordial Black Hole Formation and Abundance Estimation*, *Galaxies* **10** (2022), no. 6 112, [[arXiv:2211.13512](#)].
- [71] S. Bhattacharya, *Primordial Black Hole Formation in Non-Standard Post-Inflationary Epochs*, *Galaxies* **11** (2023), no. 1 35, [[arXiv:2302.12690](#)].
- [72] F. Ferrer, E. Masso, G. Panico, O. Pujolas, and F. Rompineve, *Primordial Black Holes from the QCD axion*, *Phys. Rev. Lett.* **122** (2019), no. 10 101301, [[arXiv:1807.01707](#)].
- [73] P. Minkowski, $\mu \rightarrow e\gamma$ at a Rate of One Out of 10^9 Muon Decays?, *Phys. Lett. B* **67** (1977) 421–428.
- [74] M. Gell-Mann, P. Ramond, and R. Slansky, *Complex Spinors and Unified Theories*, *Conf. Proc. C* **790927** (1979) 315–321, [[arXiv:1306.4669](#)].
- [75] R. N. Mohapatra and G. Senjanovic, *Neutrino Mass and Spontaneous Parity Nonconservation*, *Phys. Rev. Lett.* **44** (1980) 912.
- [76] T. Yanagida, *Horizontal Symmetry and Masses of Neutrinos*, *Prog. Theor. Phys.* **64** (1980) 1103.
- [77] J. Schechter and J. Valle, *Neutrino Masses in $SU(2) \times U(1)$ Theories*, *Phys. Rev. D* **22** (1980) 2227.

- [78] L. Di Luzio, M. Giannotti, E. Nardi, and L. Visinelli, *The landscape of QCD axion models*, *Phys. Rept.* **870** (2020) 1–117, [[arXiv:2003.01100](#)].
- [79] I. Masina, *Dark matter and dark radiation from evaporating primordial black holes*, *Eur. Phys. J. Plus* **135** (2020), no. 7 552, [[arXiv:2004.04740](#)].
- [80] S. Pascoli, S. T. Petcov, and A. Riotto, *Leptogenesis and Low Energy CP Violation in Neutrino Physics*, *Nucl. Phys. B* **774** (2007) 1–52, [[hep-ph/0611338](#)].
- [81] W. Buchmuller, P. Di Bari, and M. Plumacher, *Leptogenesis for pedestrians*, *Annals Phys.* **315** (2005) 305–351, [[hep-ph/0401240](#)].
- [82] S. Davidson, E. Nardi, and Y. Nir, *Leptogenesis*, *Phys. Rept.* **466** (2008) 105–177, [[arXiv:0802.2962](#)].
- [83] D. Borah, S. Jyoti Das, R. Samanta, and F. R. Urban, *PBH-infused seesaw origin of matter and unique gravitational waves*, *JHEP* **03** (2023) 127, [[arXiv:2211.15726](#)].
- [84] A. Pilaftsis and T. E. J. Underwood, *Resonant leptogenesis*, *Nucl. Phys. B* **692** (2004) 303–345, [[hep-ph/0309342](#)].
- [85] P. S. B. Dev, M. Garny, J. Klaric, P. Millington, and D. Teresi, *Resonant enhancement in leptogenesis*, *Int. J. Mod. Phys. A* **33** (2018) 1842003, [[arXiv:1711.02863](#)].
- [86] K. Abazajian et al., *CMB-S4 Science Case, Reference Design, and Project Plan*, [arXiv:1907.04473](#).
- [87] K. Inomata, K. Kohri, T. Nakama, and T. Terada, *Enhancement of Gravitational Waves Induced by Scalar Perturbations due to a Sudden Transition from an Early Matter Era to the Radiation Era*, *Phys. Rev. D* **100** (2019), no. 4 043532, [[arXiv:1904.12879](#)].
- [88] **LIGO Scientific** Collaboration, J. Aasi et al., *Advanced LIGO*, *Class. Quant. Grav.* **32** (2015) 074001, [[arXiv:1411.4547](#)].
- [89] **LISA** Collaboration, P. Amaro-Seoane et al., *Laser Interferometer Space Antenna*, *arXiv e-prints* (Feb., 2017) arXiv:1702.00786, [[arXiv:1702.00786](#)].
- [90] S. Kawamura et al., *The Japanese space gravitational wave antenna DECIGO*, *Class. Quant. Grav.* **23** (2006) S125–S132.
- [91] **LIGO Scientific** Collaboration, B. P. Abbott et al., *Exploring the Sensitivity of Next Generation Gravitational Wave Detectors*, *Class. Quant. Grav.* **34** (2017), no. 4 044001, [[arXiv:1607.08697](#)].
- [92] S. Sato et al., *The status of DECIGO*, *J. Phys. Conf. Ser.* **840** (2017), no. 1 012010.

- [93] T. Ishikawa et al., *Improvement of the target sensitivity in DECIGO by optimizing its parameters for quantum noise including the effect of diffraction loss*, *Galaxies* **9** (2021), no. 1 14, [[arXiv:2012.11859](#)].
- [94] J. Baeza-Ballesteros, E. J. Copeland, D. G. Figueroa, and J. Lizarraga, *Gravitational Wave Emission from a Cosmic String Loop, I: Global Case*, [arXiv:2308.08456](#).
- [95] M. Gorghetto, E. Hardy, and H. Nicolaescu, *Observing invisible axions with gravitational waves*, *JCAP* **06** (2021) 034, [[arXiv:2101.11007](#)].
- [96] A. Vilenkin, Y. Levin, and A. Gruzinov, *Cosmic strings and primordial black holes*, *JCAP* **11** (2018) 008, [[arXiv:1808.00670](#)].
- [97] M. Srednicki, *Axion Couplings to Matter. 1. CP Conserving Parts*, *Nucl. Phys. B* **260** (1985) 689–700.
- [98] **CAST** Collaboration, S. Andriamonje et al., *An Improved limit on the axion-photon coupling from the CAST experiment*, *JCAP* **04** (2007) 010, [[hep-ex/0702006](#)].
- [99] **CAST** Collaboration, V. Anastassopoulos et al., *New CAST Limit on the Axion-Photon Interaction*, *Nature Phys.* **13** (2017) 584–590, [[arXiv:1705.02290](#)].
- [100] M. S. Turner, *Axions from sn1987a*, *Phys. Rev. Lett.* **60** (May, 1988) 1797–1800.
- [101] A. Burrows, M. S. Turner, and R. P. Brinkmann, *Axions and sn 1987a*, *Phys. Rev. D* **39** (Feb, 1989) 1020–1028.
- [102] G. Raffelt and D. Seckel, *Bounds on exotic-particle interactions from sn1987a*, *Phys. Rev. Lett.* **60** (May, 1988) 1793–1796.
- [103] **Fermi-LAT** Collaboration, M. Ajello et al., *Search for Spectral Irregularities due to Photon–Axionlike-Particle Oscillations with the Fermi Large Area Telescope*, *Phys. Rev. Lett.* **116** (2016), no. 16 161101, [[arXiv:1603.06978](#)].
- [104] **ADMX** Collaboration, L. D. Duffy, P. Sikivie, D. B. Tanner, S. J. Asztalos, C. Hagmann, D. Kinion, L. J. Rosenberg, K. van Bibber, D. B. Yu, and R. F. Bradley, *A high resolution search for dark-matter axions*, *Phys. Rev. D* **74** (2006) 012006, [[astro-ph/0603108](#)].
- [105] I. Stern, *ADMX Status*, *PoS ICHEP2016* (2016) 198, [[arXiv:1612.08296](#)].
- [106] **ADMX** Collaboration, T. Braine et al., *Extended Search for the Invisible Axion with the Axion Dark Matter Experiment*, *Phys. Rev. Lett.* **124** (2020), no. 10 101303, [[arXiv:1910.08638](#)].
- [107] D. Budker, P. W. Graham, M. Ledbetter, S. Rajendran, and A. Sushkov, *Proposal for a*

- Cosmic Axion Spin Precession Experiment (CASPER)*, *Phys. Rev. X* **4** (2014), no. 2 021030, [[arXiv:1306.6089](#)].
- [108] D. Alesini, D. Babusci, D. Di Gioacchino, C. Gatti, G. Lamanna, and C. Ligi, *The KFLASH Proposal*, [arXiv:1707.06010](#).
- [109] D. Alesini et al., *KFLASH Conceptual Design Report*, [arXiv:1911.02427](#).
- [110] D. Alesini et al., *The future search for low-frequency axions and new physics with the FLASH resonant cavity experiment at Frascati National Laboratories*, *Phys. Dark Univ.* **42** (2023) 101370, [[arXiv:2309.00351](#)].
- [111] Y. Kahn, B. R. Safdi, and J. Thaler, *Broadband and Resonant Approaches to Axion Dark Matter Detection*, *Phys. Rev. Lett.* **117** (2016), no. 14 141801, [[arXiv:1602.01086](#)].
- [112] J. L. Ouellet et al., *First Results from ABRACADABRA-10 cm: A Search for Sub- μeV Axion Dark Matter*, *Phys. Rev. Lett.* **122** (2019), no. 12 121802, [[arXiv:1810.12257](#)].
- [113] S. Lee, S. Ahn, J. Choi, B. R. Ko, and Y. K. Semertzidis, *Axion Dark Matter Search around $6.7 \mu\text{eV}$* , *Phys. Rev. Lett.* **124** (2020), no. 10 101802, [[arXiv:2001.05102](#)].
- [114] Y. K. Semertzidis et al., *Axion Dark Matter Research with IBS/CAPP*, [arXiv:1910.11591](#).
- [115] **MADMAX Working Group** Collaboration, A. Caldwell, G. Dvali, B. Majorovits, A. Millar, G. Raffelt, J. Redondo, O. Reimann, F. Simon, and F. Steffen, *Dielectric Haloscopes: A New Way to Detect Axion Dark Matter*, *Phys. Rev. Lett.* **118** (2017), no. 9 091801, [[arXiv:1611.05865](#)].
- [116] J. K. Vogel et al., *IAXO - The International Axion Observatory*, in *8th Patras Workshop on Axions, WIMPs and WISPs*, 2, 2013. [arXiv:1302.3273](#).
- [117] **IAXO** Collaboration, E. Armengaud et al., *Physics potential of the International Axion Observatory (IAXO)*, *JCAP* **06** (2019) 047, [[arXiv:1904.09155](#)].
- [118] M. Meyer, M. Giannotti, A. Mirizzi, J. Conrad, and M. A. Sánchez-Conde, *Fermi Large Area Telescope as a Galactic Supernovae Axionscope*, *Phys. Rev. Lett.* **118** (2017), no. 1 011103, [[arXiv:1609.02350](#)].
- [119] V. Cardoso, O. J. C. Dias, G. S. Hartnett, M. Middleton, P. Pani, and J. E. Santos, *Constraining the mass of dark photons and axion-like particles through black-hole superradiance*, *JCAP* **03** (2018) 043, [[arXiv:1801.01420](#)].
- [120] **TASTE** Collaboration, V. Anastassopoulos et al., *Towards a medium-scale axion helioscope and haloscope*, *JINST* **12** (2017), no. 11 P11019, [[arXiv:1706.09378](#)].

- [121] R. T. Co, L. J. Hall, and K. Harigaya, *QCD Axion Dark Matter with a Small Decay Constant*, *Phys. Rev. Lett.* **120** (2018), no. 21 211602, [[arXiv:1711.10486](#)].
- [122] R. T. Co, L. J. Hall, K. Harigaya, K. A. Olive, and S. Verner, *Axion Kinetic Misalignment and Parametric Resonance from Inflation*, *JCAP* **08** (2020) 036, [[arXiv:2004.00629](#)].
- [123] S. Ramazanov and R. Samanta, *Heating up Peccei-Quinn scale*, *JCAP* **05** (2023) 048, [[arXiv:2210.08407](#)].
- [124] S. Dodelson and L. M. Widrow, *Sterile-neutrinos as dark matter*, *Phys. Rev. Lett.* **72** (1994) 17–20, [[hep-ph/9303287](#)].
- [125] M. Drewes et al., *A White Paper on keV Sterile Neutrino Dark Matter*, *JCAP* **01** (2017) 025, [[arXiv:1602.04816](#)].
- [126] D. K. Ghosh, A. Ghoshal, and S. Jeusun, *Axion-like particle (ALP) portal freeze-in dark matter confronting ALP search experiments*, *JHEP* **01** (2024) 026, [[arXiv:2305.09188](#)].
- [127] A. Bharucha, F. Brümmer, N. Desai, and S. Mutzel, *Axion-like particles as mediators for dark matter: beyond freeze-out*, *JHEP* **02** (2023) 141, [[arXiv:2209.03932](#)].
- [128] P. J. Fitzpatrick, Y. Hochberg, E. Kuflik, R. Ovadia, and Y. Soreq, *Dark matter through the axion-gluon portal*, *Phys. Rev. D* **108** (2023), no. 7 075003, [[arXiv:2306.03128](#)].
- [129] D. Borah, S. Jyoti Das, and A. K. Saha, *Cosmic inflation in minimal $U(1)_{B-L}$ model: implications for (non) thermal dark matter and leptogenesis*, *Eur. Phys. J. C* **81** (2021), no. 2 169, [[arXiv:2005.11328](#)].
- [130] A. Datta, R. Roshan, and A. Sil, *Imprint of the Seesaw Mechanism on Feebly Interacting Dark Matter and the Baryon Asymmetry*, *Phys. Rev. Lett.* **127** (2021), no. 23 231801, [[arXiv:2104.02030](#)].
- [131] K. Griest and M. Kamionkowski, *Unitarity Limits on the Mass and Radius of Dark Matter Particles*, *Phys. Rev. Lett.* **64** (1990) 615.
- [132] G. F. Giudice, E. W. Kolb, and A. Riotto, *Largest temperature of the radiation era and its cosmological implications*, *Phys. Rev. D* **64** (2001) 023508, [[hep-ph/0005123](#)].